One Health Advances

ARTICLE

Open Access

Development of a lateral flow immunochromatography assay for the detection of fluoroacetamide in blood samples

Qiang Li[1], Ling Yang[1,2], Changfei Duan[1], Xiaonan Wang[1] and Xuezhi Yu[1*]

Abstract

Fluoroacetamide (FAM) has been employed as a rodenticide for an extended duration, leading to a multitude of incidents involving human ingestion poisoning. Currently, FAMs have been prohibited by nations globally; however, there are still instances of their illegal usage. Conventional instrument methods are characterized by their time-consuming nature and complex operational procedures, rendering them inadequate for meeting urgent diagnostic needs in patients with acute FAM poisoning. Therefore, there is an immediate need to develop a prompt, user-friendly, and precise immunoassay method for the diagnosis of acute poisoning induced by FAM. A lateral flow immunochromatography assay (LFIA) was developed in this study for the visual detection of FAMs in blood samples, representing the first report of such an approach. The method exhibited a cut-off value of 0.5 mg/mL under the optimized conditions, enabling the entire FAM detection process in blood samples to be completed within a mere 8 min without any pretreatment requirements. Notably, the results were easily discernible by visual inspection alone. These results indicate that the developed LFIA holds great promise as a convenient and rapid diagnostic tool for FAM poisoning diagnosis, thereby offering valuable support for subsequent treatment strategies.

Keywords Fluoroacetamide, Rodenticide, Lateral flow immunochromatography assay, Blood samples

Introduction

As a highly toxic fluorinated compound, fluoroacetamide (FAM) is water soluble, tasteless, odorless, and stable, rendering it suitable for use as an insecticide [1, 2] or rodenticide. FAM and its metabolite fluoroacetic acid (FAA) were extensively employed in the last century in the United States and New Zealand to control invasive species and curb overbreeding [3, 4]. The pronounced toxicity of FAM arises from its ability to impede the tricarboxylic acid cycle (the Krebs cycle) through conversion into fluoroacetic acid within living organisms. This conversion leads to the formation of fluoroacetyl-enzyme A (CoA) through the combination of fluoroacetic acid and CoA, subsequently resulting in the production of fluorocitric acid instead of citrate. Consequently, cell metabolism disorders ensue along with systemic poisoning [5–7]. The lethal concentrations of FAMs vary among different animal species, with rats exhibiting a toxicity threshold of 15 mg/kg when FAMs are administered orally [8]. The range

*Correspondence:
Xuezhi Yu
yu51422396@126.com
[1] National Key Laboratory of Veterinary Public Health and Safety, Beijing Key Laboratory of Detection Technology for Animal Derived Food Safety, Beijing Laboratory for Food Quality and Safety, College of Veterinary Medicine, China Agricultural University, Beijing 100193, People's Republic of China
[2] Department of Food and Bioengineering, Beijing Vocational College of Agriculture, Beijing 102442, People's Republic of China

for humans is reported to be between 2 and 10 mg/kg [5]. The global incidence of FAM poisoning in humans [9, 10], domestic animals [11, 12], and wildlife [13] has been extensively documented due to its pronounced toxic effects on most mammalian organisms. In the case of rodenticide poisoning, accidental ingestion was the most common cause of poisoning in children, and intentional ingestion and unknown intake were the most frequent causes in adults [10]. By the end of the previous century, nations worldwide had implemented prohibitions on the manufacturing and commercialization of FAMs as pesticides. Due to the appealing advantages of FAMs, such as uncomplicated preparation technology, cost effectiveness, and commendable deratization efficacy, there is a substantial prevalence of illicit production and utilization of FAMs as rodenticides. This unfortunate circumstance frequently results in human ingestion poisoning, which is particularly prevalent within developing nations such as China [14]. In 2022, news reports continued to emerge regarding the tragic death of a 10-year-old Chinese girl due to poisoning caused by the consumption of bread contaminated with FAMs. Therefore, there is an urgent need to develop an expeditious and highly sensitive detection technique for the prompt diagnosis of acute FAM poisoning.

Currently, the majority of FAM detection methods rely on instruments. Numerous analytical techniques utilizing gas chromatography–mass spectrometry (GC–MS) [15–19] and ultrahigh-performance liquid chromatography (UPLC) [20, 21] have been established and employed for FAM detection. These methods exhibit relatively high sensitivity and specificity; however, they are dependent on costly equipment, skilled operators, and a time-consuming and complex sample pretreatment process. Consequently, the practicality of these methods for on-site detection is limited, and there are no reports or products for rapid detection of FAM currently.

As a rapid detection method, immunoassays could meet the demand of on-site detection of FAMs. Among all immunoassays, the lateral flow immunochromatography assay (LFIA) has emerged as the most attractive tool for fast on-site detection owing to its inherent advantages, including a straightforward pretreatment process, obviating the need for costly instrumentation and specialized expertise, and yielding prompt visual detection outcomes. However, there are no reports about LFIAs for FAMs detection. The reason is that the molecular weight of FAM is only 77 Da, which may not be enough to make even a single epitope. It is very difficult and challenging to produce a specific monoclonal antibody (mAb) against FAM. However, mAbs are key reagents for immunoassays. Fortunately, our group has dedicated extensive efforts to the development of antibodies targeting small molecule haptens over an extended period. Recently, our group employed a de novo synthesis strategy to design and synthesize FAM haptens. Furthermore, successful preparation of the mAb 5D11 against FAM was achieved through the immunization of mice for the first time [22].

Herein, the aim of this study was to construct an LFIA method based on gold nanoparticle (AuNP)-labeled mAb 5D11 (AuNP-mAb) for the detection of FAMs in blood samples. This method represents rapid progress toward fast FAM detection and is a practical diagnostic method for acute FAM poisoning.

Results

The principle of LFIA based on AuNPs-mAb

A schematic of the developed LFIA based on AuNPs-mAb was depicted in Fig. 1. The test strip consisted

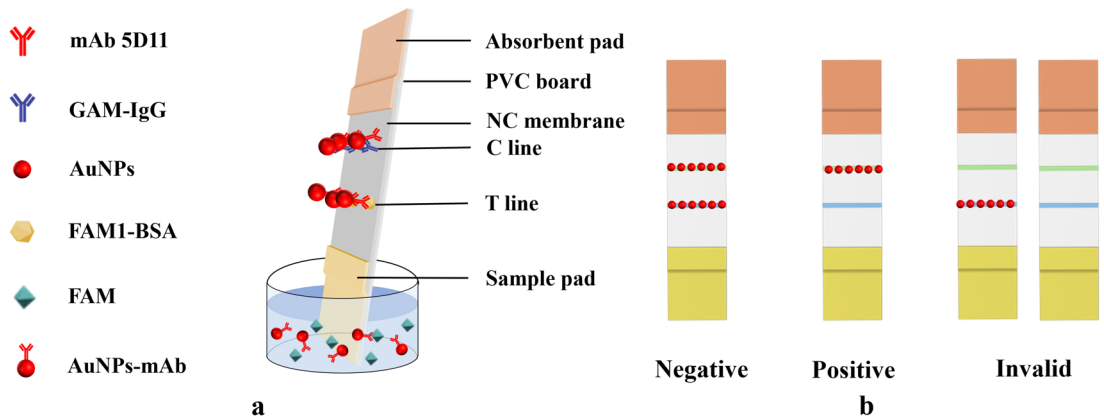

Fig. 1 Schematic of the developed LFIA. (**a**) The component and test procedure of the strip. (**b**) Schematic of the test results, including negative, positive and invalid results, from left to right

of six distinct sections, namely, a PVC board, an NC membrane, an absorbent pad, a sample pad, a test line (T line) coated with the coating antigen FAM1-BSA, and a control line (C line) coated with goat anti-mouse IgG (GAM-IgG), as shown in Fig. 1a. When the test strip is inserted into a sample containing the FAM target and AuNP-mAb probe solution, if the concentration of FAM in the sample exceeds the threshold (indicating a positive sample), all of the AuNP-mAbs will bind with FAM instead of the coating antigen FAM1-BSA on the T line, resulting in an absence of color on the T line. Conversely, if the concentration of FAM in the sample solution falls below this threshold (indicating a negative sample), the AuNPs-mAb will be captured by FAM1-BSA on the T line, resulting in a red-colored T line. In either case, unless there is an issue with strip validity, the AuNPs-mAb will always be captured by GAM-IgG on the C line (Fig. 1b).

Preparation and parameter optimization of the AuNP-mAb probe

AuNPs were synthesized through the reduction of $HAuCl_4$ using sodium citrate under boiling conditions, resulting in a visually appealing transparent wine red when observed under natural light. According to the transmission electron microscopy (TEM) image (Fig. 2a), the AuNPs were monodisperse particles with an average diameter of approximately 30 nm. As shown in the UV–Vis absorption spectrum (Fig. 2c), the resonance absorption peak of the AuNPs appeared at 530 nm and shifted to 535 nm after coating with mAb 5D11, which indicated the formation of the AuNP–mAb 5D11 signal probe. In general, AuNPs typically exhibit a negative surface charge due to the presence of citrate ligands [23], while IgG is known for its positively charged surface [24]. Consequently, coating these positively charged antibodies onto negatively charged AuNPs leads to a reduction in the *zeta* potential of the AuNPs (here, this change refers to the absolute value of the *zeta* potential). Figure 2d shows that the *zeta* potential of the AuNPs changed from −35.2 mV

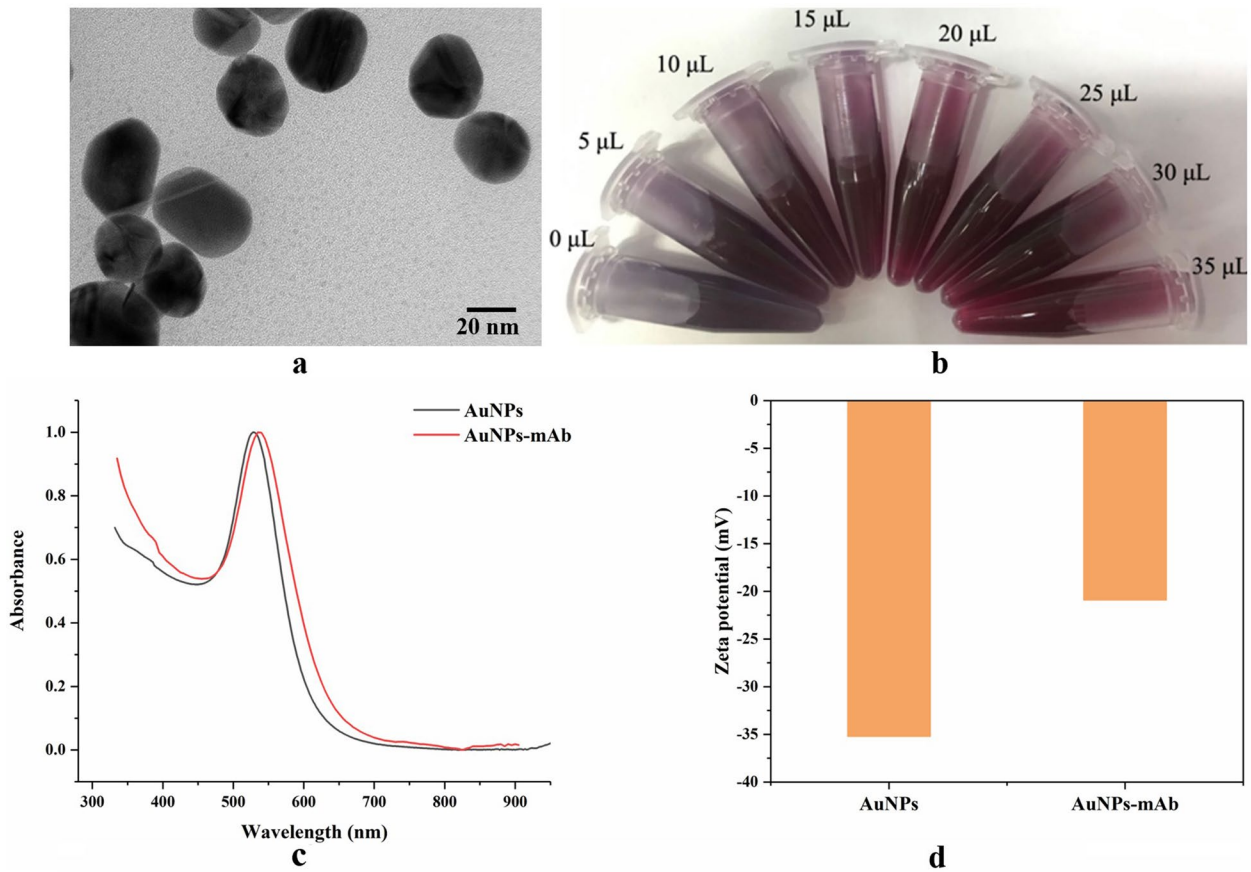

Fig. 2 Characterization of AuNPs and the AuNP-mAb probe. (**a**) Transmission electron microscopy (TEM) images of AuNPs with scale bars of 20 nm. (**b**) The color of the colloidal gold solution with different volumes of K_2CO_3. (**c**) UV–Vis absorption spectra of the AuNPs and the AuNP-mAb probe. (**d**) The *zeta* potentials of the AuNPs and the AuNP-mAb probe

to −20.9 mV after coating with the mAb 5D11, which further confirmed that the AuNP-mAb probe was successfully prepared.

Several crucial parameters play pivotal roles in the production of AuNP-mAb probes during the labeling procedure, including the pH, mAb 5D11 volume, antibody diluents, and colloidal gold probe resuspension solution. We adjusted the pH of the AuNP solution by adding different amounts of K_2CO_3; the colloidal gold solution maintained its wine-red color when the volume of K_2CO_3 exceeded 15 μL (Fig. 2b), while it transitioned from gray to purple when the volume of K_2CO_3 did not exceed 15 μL. The colloidal gold probe produced by the addition of 15 or 20 μL of K_2CO_3 was subsequently tested via LFIA (Fig. 3a). The results indicated that the T line exhibited enhanced clarity and superior inhibition of FAM when supplemented with a volume of 15 μL of K_2CO_3. The volume of the mAb 5D11 influences the signal intensity and sensitivity of the LFIA. According to the signal intensity of the different volumes of added antibody (Fig. 3b), the color intensity of the T line gradually increased with increasing antibody concentration but decreased when the amount of antibody was greater than 100 μL. Figure 3c shows the signal intensity and inhibitory effect of the LFIA strip upon the addition of different volumes of antibody. The T line had the brightest signal for a negative sample and a greater inhibitory effect for the FAM-containing samples when the volume of mAb 5D11 was 80 μL. To ensure optimal signal intensity for negative samples while maintaining superior inhibitory sensitivity for positive samples, an antibody volume of 80 μL was recommended.

BSA is commonly added to antibody diluents to enhance probe stability and reduce nonspecific binding. We compared the LFIA performance of different concentrations of BSA solution as an antibody diluent. As shown in Fig. 4a, the specific signal on the T line was also blocked completely due to the high concentration of 10% BSA. Conversely, a lower concentration (0.5%) of BSA demonstrated superior signal intensity and inhibitory effect with minimal background interference for both the negative and FAM-containing samples. The stability and chromatographic performance of the AuNPs-mAb probe are significant and influenced by the resuspension

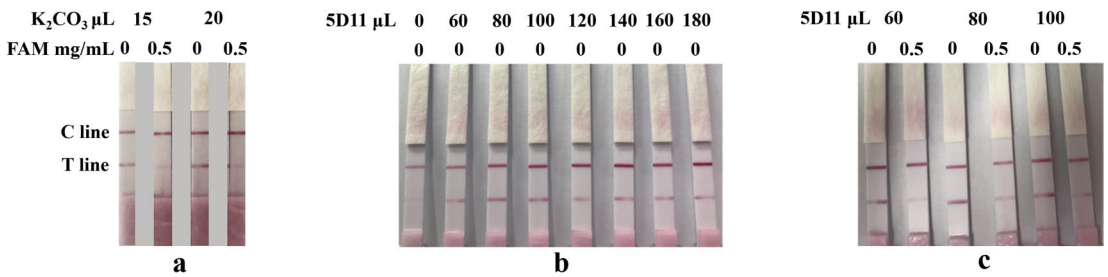

Fig. 3 Optimization results of the volume of K_2CO_3 and mAb 5D11 for the preparation of the AuNP-mAb probe. (**a**) Chromatographic results for negative samples and positive samples detected by AuNP probes prepared with 15 and 20 μL of K_2CO_3 (right). (**b**) Chromatographic results of the prepared AuNP–mAb probes with different volumes of the mAb 5D11 and (**c**) contrastive results for the negative and positive samples. Negative samples: blood samples that did not contain FAMs; positive samples: blood samples with 0.5 mg/mL FAMs

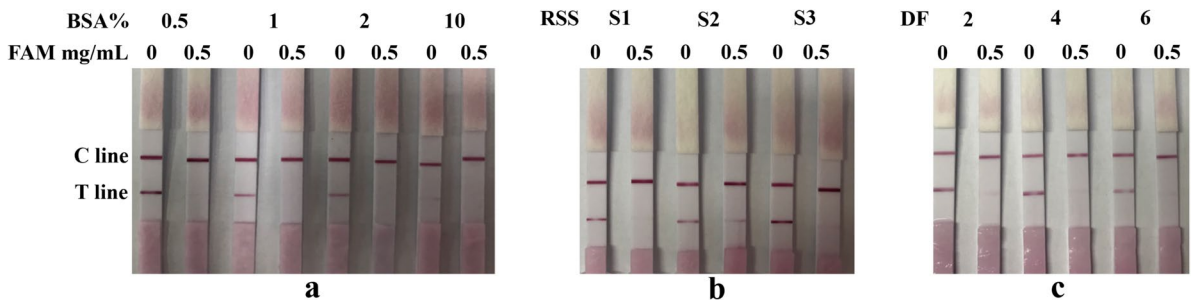

Fig. 4 Optimization results for the antibody diluents, resuspension solution of the AuNP-mAb probe (abbreviated as RSS) and dilution factor of the coating antigen (abbreviated as DF). (**a**) Chromatographic results for negative samples and positive samples tested with AuNP probes prepared with different antibody diluents. (**b**) Chromatographic results for negative samples and positive samples tested with AuNP probes prepared with different resuspension solutions. (**c**) Chromatographic results for the negative samples and positive samples tested by strips prepared with different concentrations of coating antigen. Negative samples: blood samples that did not contain FAMs; positive samples: blood samples with 0.5 mg/mL FAMs

solution. To evaluate the performance of the LFIA, three solutions (S1, S2, and S3) were selected as resuspension solutions. The LFIA results, depicting the performance of the AuNP probes in different resuspension solutions, are presented in Fig. 4b. Notably, when S2 was used as the resuspension solution, the strip exhibited the lowest signal intensity and inhibition effect. Conversely, a strip utilizing resuspension solution S3 had the brightest T line and demonstrated superior sensitivity. Consequently, S3 was selected as the optimal resuspension solution for the AuNP-mAb probe in LFIA assays.

Optimization of the coating antigen concentration

As an immunoassay based on the antigen–antibody reaction, binding between a coating antigen and an antibody significantly influences both the color intensity and sensitivity of LFIAs. Consequently, we conducted optimization experiments to determine the optimal concentration of coating antigen on the T line by employing 2-, 4-, and sixfold diluted FAM1-BSA solutions. According to the results in Fig. 4c, when FAM1-BSA was diluted by a factor of 2, the T line exhibited the most intense red color for the negative samples and demonstrated comparable sensitivity in detecting FAM-containing samples when compared to dilutions of FAM1-BSA by factors of 4 and 6. Consequently, we selected a twofold diluted solution of FAM1-BSA as the coating antigen on the T line.

Optimization of the NC membrane and sample pad

The sensitivity of LFIA can be influenced by the porosity and protein binding affinity of the NC membrane. In general, a decrease in pore size leads to a reduction in the flow rate of reaction liquid through the membrane, consequently resulting in an extended reaction time. In this section, we conducted a comparative analysis of three types of NC membranes with varying pore sizes as chromatographic carriers. As depicted in Fig. 5a, the MDI90 NC membrane did not exhibit any red signal on the T line for either the positive or negative samples. Conversely, both the Sartorius 95 (S95) NC membrane and the Millipore 135 (M135) NC membrane demonstrated sensitive inhibitory effects. However, it is noteworthy that the M135 NC membrane displayed a brighter signal on the T line for negative samples. Consequently, considering these observations, we selected the M135 NC membrane as our preferred choice for chromatographic carriers. The material of the sample pad influences the immunochromatographic speed and the release speed of the AuNP-mAb probe. According to the test results for three sample pads with different materials (Fig. 5b), SB08 exhibited a faster release speed. However, during the chromatographic process, there was inconsistency in the chromatographic speed, leading to an uneven T line signal for the negative samples. Additionally, the strip with the RB65 sample pad displayed a pale C line signal and no red signal on the T line. Finally, the sample pad for LFIA was chosen for use in whole-blood separation membrane (WBSM) due to its superior signal uniformity and sensitivity.

Optimization of the reaction conditions

The optimization of sample volume, AuNP-mAb probe volume, and chromatographic time is crucial for achieving optimal performance in LFIA. We optimized these three parameters by adjusting the volume of the AuNP-mAb probe to 2, 4, or 6 μL; the sample volume to 100, 150, or 200 μL; and the chromatographic time to 3, 5, or 8 min, respectively. Subsequently, we determined the optimal reaction conditions based on signal intensity and sensitivity (keeping all positive samples at a consistent FAM concentration of 0.5 mg/mL). All the test results are summarized in Table 1. With increasing sample volume,

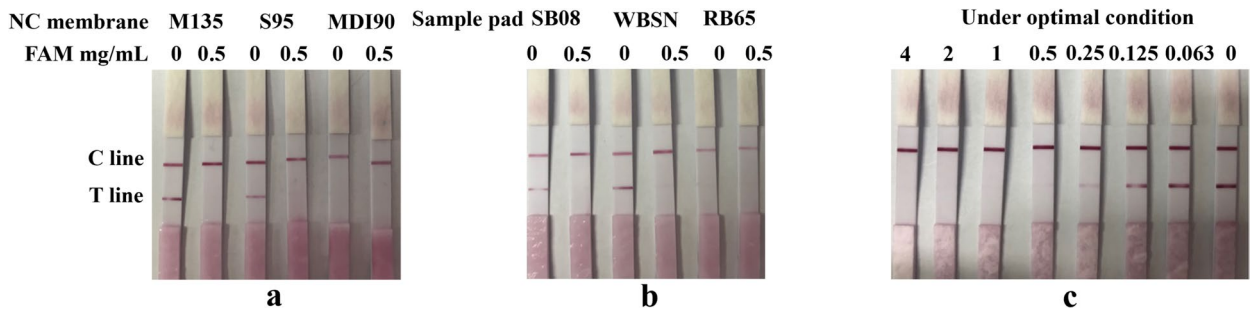

Fig. 5 Optimization results of the NC membrane and sample pad and the cut-off value. (**a**) Chromatographic results for negative samples and positive samples tested by strips prepared with different NC membranes. (**b**) Chromatographic results for negative samples and positive samples tested by strips prepared with different sample pads. (**c**) Chromatographic results for blood samples containing different concentrations of FAMs, as tested by the developed LFIA under optimal conditions. Note: Negative samples: blood samples that do not contain FAMs; Positive samples: blood samples with 0.5 mg/mL FAMs

Table 1 Optimization results for the AuNP-mAb probe volume, sample volume and chromatographic time

group	AuNPs probe volume (μL)	sample volume (μL)	chromatographic time (min)	signal intensity of negative samples	signal intensity of positive samples
1	2	100	3	+	-
2	2	150	3	+	-
3	2	200	3	+ +	-
4	4	100	5	+ +	+
5	4	150	5	+ + +	-
6	4	200	5	+ + + +	+
7	6	100	8	+ + + +	+
8	6	150	8	+ + + +	+ +
9	6	200	8	+ + + + +	+ +

The amount of "+" represents the brightness of the red signal on the T line, and "-" represents no red signal on the T line

AuNP-mAb probe volume, and chromatographic time, the signal intensity on the T line of the negative samples increased. Conversely, the inhibitory effect on the positive samples decreased. After careful evaluation, we determined that the optimal reaction conditions consisted of 150 μL of sample, 4 μL of AuNP-mAb probe, and a chromatographic time of 5 min. These conditions were chosen because they successfully achieved complete inhibition of the T-line signal for positive samples while yielding the highest T-line signal intensity for negative samples under these circumstances.

Evaluation of LFIA strip performance

First, blood samples with varying concentrations of FAMs (ranging from 0 to 4 mg/mL in increments of 0.063) were subjected to testing under the optimized conditions. Subsequently, the cut-off value was determined as the FAM concentration at which the T-line signal completely disappeared, indicating the minimum visually detectable concentration of the established LFIA. As shown in Fig. 5c, the signal on the T line disappeared when the FAM concentration reached 0.25 mg/mL, and its disappearance became distinctly visible to the naked eye at a FAM concentration of 0.5 mg/mL. Consequently, we determined that 0.5 mg/mL served as the cut-off value for the established LFIA in blood samples. Subsequently, the established LFIA was employed to examine 30 negative blood samples and 30 positive blood samples under optimal conditions. Remarkably, only one positive result was detected among all the negative samples, while no negative result was observed in any of the positive samples. These findings indicate a false positive rate of approximately 3.3% and an impeccable false negative rate of 0%. All the results suggest that the developed LFIA exhibits exceptional accuracy and reproducibility, suggesting that it is a valuable diagnostic tool for rapid and convenient detection of acute poisoning caused by FAM.

Discussion

The illicit utilization of FAMs remains pervasive, leading to frequent occurrences of ingestion poisoning in both humans and animals. The primary challenge lies in promptly diagnosing FAM poisoning to facilitate subsequent treatment interventions. Despite the development of numerous instrument-based laboratory testing methods, their prolonged detection time fails to satisfy the demand for rapid clinical screening. Analysis based on specific recognition elements is deemed more suitable for clinical field detection. To date, only two FAM-specific recognition elements have been reported, encompassing a DNA aptamer that remains unexplored in actual detection and a monoclonal antibody meticulously prepared by our group [8, 22]. In this study, to address the pressing demand for on-site detection of FAMs, for the first time, we developed an LFIA based on antigen–antibody binding for rapid diagnosis of FAM poisoning in blood samples.

Despite the high sensitivity of instrumental analysis methods (Table 2), such as GC–MS and UPLC [15–18], intricate preprocessing procedures that involve derivatization, extraction, and concentration are needed. The

Table 2 Comparison of the developed LFIA with other methods

Detection method	Sample	LOD	Detection time
GC–MS [15]	Drinking water	0.15 μg/L	3 h
SPME-GC–MS [16]	Blood sample	1 mg/L	/
GC–MS [18]	Fresh pork	0.08 mg/kg	/
This research	Blood sample	0.5 mg/mL	8 min

entire detection process often spans several hours or even days and relies on a laboratory environment that adheres to rigorous standards to ensure accuracy and reliability. In contrast, the developed LFIA demonstrated exceptional accuracy in directly detecting untreated blood samples under ideal conditions. Moreover, the detection results can be visually interpreted within a mere 8 min by the naked eye, enabling prompt diagnosis of patients with FAM poisoning upon admission.

Given the challenging nature of preparing specific monoclonal antibodies for the ultrasmall molecule FAM, the sensitivity of the developed LFIA may be relatively low. Nonetheless, this study successfully addresses a critical gap in rapid FAM detection through immunoassays. Furthermore, this work serves as an impetus to develop more sensitive FAM-specific monoclonal antibodies and enhance the overall sensitivity of LFIAs. Moreover, there is potential for applying this detection method to environmental and food samples, thereby monitoring the illegal use of FAMs and ensuring food safety.

Conclusion

In this study, for the first time, we successfully developed an LFIA based on the AuNP-labeled mAb 5D11 for rapid and on-site detection of FAMs in blood samples. By optimizing the experimental conditions, we achieved qualitative detection of FAMs with a cut-off value of 0.5 mg/mL, and the results could be visually read within a mere 8 min through direct observation without the need for specialized equipment or instruments, making this a rapid and cost-effective method. As the first developed rapid detection method for FAM, this work provides substantial support for the convenient and expeditious diagnosis of acute FAM poisoning in clinical settings.

Materials and methods

Chemical reagents and instruments

Gold(III) chloride hydrate, potassium carbonate, sulfuric acid, nitric acid, and sodium citrate were obtained from Sinopharm Chemical Reagent Co., Ltd. (Shanghai, China). Bovine serum albumin (BSA) was purchased from Sigma–Aldrich (St. Louis, MO, USA). The mAb 5D11 and coating antigen FAM1-BSA were prepared in our own laboratory. Goat anti-mouse IgG was purchased from Jackson ImmunoResearch Laboratories, Inc. Human blank blood was obtained from Beijing WDWK Biotech Co., Ltd. (Beijing, China). The FAM standard substance was obtained from Dr. Ehrenstorfer Co., Ltd. (Augsburg, Germany). The Millipore 135 NC membrane was obtained from Millipore Corporation (MA, USA). Sartorius 95 NC membranes were obtained from Sartorius Stedim Biotech (Goettingen, Germany). The MDI 90 NC membrane was obtained from Advanced Microdevices Pvt. Ltd. (Ambala Cantt., India). The SB08 sample pad, RB65 sample pad, WBSM (whole blood separation membrane) sample pad, and PVC board were obtained from Shanghai Gold Bio Technology Co., Ltd. (Shanghai, China). The absorbent pad was obtained from Shanghai Liangxin Co., Ltd. (Shanghai, China). Colloidal gold probe resuspension solutions S1, S2, and S3 were obtained from Beijing WDWK Biotech Co., Ltd. (Beijing, China).

A cantilever agitator was obtained from IKA (Guangzhou) Instrument Equipment Co., Ltd. (Guangzhou, China). The *zeta* potential was measured by a Zetasizer Nano ZS90 (Malvern Panalytical, UK). The XYZ platform dispenser HM3030 and strip cutter ZQ 2000 were obtained from Shanghai Gold Bio Technology Co., Ltd. (Shanghai, China).

The preparation and characterization of AuNPs

AuNPs were prepared by reducing Gold(III) chloride hydrate with sodium citrate under boiling conditions. The conical flask and magnetic rotors were presoaked in aqua regia for 24 h and then washed with deionized water. One milliliter of 1% chloroauric acid solution was added to 100 mL of deionized water under continuous stirring and heating until the solution boiled. Subsequently, 2 mL of 1% sodium citrate was added quickly, and the mixture was stirred and heated for 10 min until the solution was wine red. The solution was cooled to room temperature and stored at 4 °C. Finally, transmission electron microscopy (TEM) and spectrophotometry were used to characterize the morphologies and optical characteristics of the prepared AuNPs.

Fabrication and parameter optimization of the AuNP-mAb probe

The AuNP-mAb probe was fabricated via electrostatic adsorption between AuNPs and the mAb 5D11. One milliliter of AuNP solution was added to a tube, and then a certain amount of potassium carbonate was added to adjust the pH of the solution. Next, 100 times diluted mAb 5D11 solution was gently added to the pH-adjusted AuNP solution, and the mixture was reacted for 10 min at room temperature to form the AuNP-mAb probe. After that, 20 μL of 20% BSA solution was added and reacted for 10 min at room temperature to block the unbinding site. Finally, the mixture was centrifuged at 10,000 rpm at 4 °C for 10 min, after which the precipitate at the bottom of the tube was resuspended in 200 μL of resuspension solution. We also measured the surface *zeta* potential of the AuNPs before and after reaction with the mAb 5D11 by a Zetasizer Nano ZS90 to confirm the results.

The optimization of pH was performed by changing the volume of 0.1 M potassium carbonate to 0, 5, 10, 15, 20,

25, 30, or 35 μL when it was added to 1 mL of AuNP solution (the volume of mAb 5D11 was fixed at 20 μL); other steps, such as those above, were not repeated. According to the solution color, two suitable potassium carbonate volumes were selected to prepare the AuNP-mAb probe. These two probes were subsequently tested for negative samples and positive samples by LFIA. Finally, the optimal potassium carbonate concentration was selected according to the highest T-line signal intensity for the negative samples and the greatest inhibition effect for the positive samples.

The optimization of the amount of mAb 5D11 was performed by changing the volume of the mAb to 0, 60, 80, 100, 120, 140, 160, or 180 μL during the process of fabricating AuNP probes (the volume of 0.1 M potassium carbonate was fixed at 15 μL); other steps, such as those above, were not repeated. All of these AuNP probes were tested for negative samples and positive samples by LFIA. The optimal amount of the mAb 5D11 was selected according to the highest T-line signal intensity for negative samples and the best inhibition effect for positive samples.

To screen suitable antibody diluents and probe resuspension solutions, we fabricated AuNP probes by diluting mAb 5D11 with 0.5%, 1%, 2%, and 10% BSA solutions. Then, the precipitates of the AuNP-mAb probes were resuspended in S1, S2, and S3 solutions. The AuNPs-mAb probes obtained under different antibody diluents and probe resuspension solutions were used to test negative samples and positive samples by LFIA. The optimal antibody diluents and probe resuspension solution were selected because they had the highest T line signal intensity for the negative samples and the best inhibition effect for the positive samples.

Optimization of the coating antigen concentration

Briefly, 2, 4, and 6 times diluted FAM1-BSA (10 mg/mL) in 0.01 M PB (phosphate buffer solution, pH 7.4) was sprayed uniformly on the T line of the strips and dried at 37 °C for 2 h. Then, all of the strips were used to test negative samples and positive samples by LFIA. The optimal FAM1-BSA concentration was selected according to the highest T-line signal intensity for negative samples and the best inhibition effect for positive samples.

Optimization of the NC membrane and sample pad

FAM1-BSA and GAM-IgG were sprayed uniformly on the T line and C line of three different NC membranes, namely, M135 (Millipore 135), S95 (Sartorius 95), and MDI90. The three different assembled NC membrane strips were used for the detection of negative samples and positive samples, and the optimal NC membrane was selected because it had the highest T line signal intensity for negative samples and the best inhibition effect for positive samples. To choose a suitable sample pad, we assembled strips using SB08, WBSM (whole blood separation membrane), and RB65; subsequently, these strips were used to test negative samples and positive samples by LFIA. The optimal sample pad was selected according to the highest T line signal intensity for negative samples and the best inhibition effect for positive samples.

Optimization of chromatographic conditions

The key factors that affect the signal intensity and sensitivity in chromatographic processes include the sample volume, AuNP probe volume, and chromatographic time. A total of 9 groups of tests were designed to optimize these three parameters, and each group of tests included one negative sample and one positive sample. The detailed grouping is shown in Table 3. By comparing the LFIA results of these 9 groups, the group with the highest signal intensity, best inhibition effect, lowest background noise and shortest chromatographic time was selected as the best chromatographic conditions.

Strip assembly and test procedure

First, two dilutions of FAM1-BSA and GAM-IgG at the appropriate concentrations were sprayed on a Millipore 135 NC membrane at a speed of 0.8 μL/cm as the test line and the control line (T line and C line, respectively). After that, the dry NC membrane was affixed to the middle position of the PVC board, and then the sample pad and the absorbent pad were attached to both ends of the PVC board; the sample pad was covered with an NC membrane of approximately 2 mm, and the absorbent pad was covered with an NC membrane of approximately 1 mm. Finally, the whole module was cut into 4 mm wide strips by a ZQ 2000 strip cutter and stored in a sealed bag with desiccant.

Table 3 Detailed group information for optimizing the sample volume, AuNP-mAb probe volume and chromatographic time

Group	AuNPs-mAb probe volume (μL)	sample volume (μL)	chromatographic time (min)
1	2	100	3
2	2	150	3
3	2	200	3
4	4	100	5
5	4	150	5
6	4	200	5
7	6	100	8
8	6	150	8
9	6	200	8

The entire test process was carried out in a microcell. First, 150 μL of blood sample and 4 μL of the AuNP-mAb probe were added to a microwell with full mixing; after incubating for 3 min, the sample pad of the assembled strip was inserted into the microwell for 5 min. Finally, there was a visual signal from the naked eye on the T line.

Acknowledgements
Not applicable.

Authors' contributions
Q.L. contributed to the development of the LFIA and original draft preparation; L.Y. mainly completed the preparation and optimization of the AuNPs-mAb probe; C.D. mainly performed the test of various samples and revised parts of the manuscripts; X.W. optimized the reaction condition and revised parts of the manuscripts; X.Y. guided the idea design of the LFIA and the overall revision of the manuscript. All authors read and approved the final manuscript.

Funding
This work was supported by Beijing Municipal Science and Technology Commission (Z211100007021007), the earmarked fund for CARS36, the Key R&D Program of Ningxia Hui Autonomous Region (2021BBF02036), and the program of Beijing Municipal Education Commission (KM202212448002).

Availability of data and materials
Data will be shared upon request by the readers.

Declarations

Ethics approval and consent to participate
Not applicable.

Consent for publication
Not applicable.

Competing interests
The authors declare no conflict of interest.

Received: 27 December 2023 Revised: 13 February 2024 Accepted: 29 February 2024
Published online: 25 March 2024

References

1. David WAL, Gardiner BOC. Fluoroacetamide as a systemic insecticide. Nature. 1958;181(4626):1810. https://doi.org/10.1038/1811810a0.
2. Matsumura F, O'Brien RD. A comparative study of the modes of action of fluoroacetamide and fluoroacetate in the mouse and american cockroach. Biochem Pharmacol. 1963;12(10):1201–5. https://doi.org/10.1016/0006-2952(63)90095-9.
3. Eason C, Miller A, Ogilvie S, Fairweather A. An updated review of the toxicology and ecotoxicology of sodium fluoroacetate (1080) in relation to its use as a pest control tool in New Zealand. New Zeal J Ecol. 2011;35(1):1–20.
4. Parkes JP, Nugent G, Morriss GA. Effects of aerial 1080 operations on deer populations in New Zealand. New Zeal J Ecol. 2020;44(2):3417. https://doi.org/10.20417/nzjecol.44.21.
5. Proudfoot AT, Bradberry SM, Vale JA. Sodium fluoroacetate poisoning. Toxicol Rev. 2006;25(4):213–9. https://doi.org/10.2165/00139709-200625040-00002.
6. David WAL, Gardiner BOC. Persistence of fluoroacetate and fluoroacetamide in soil. Nature. 1966;209(5030):1367–8. https://doi.org/10.1038/2091367b0.
7. Liu L, Li F, Dong Z, Dong G, Xu J, Liu W, et al. Plasma fluoroacetic acid concentrations: symptoms, hematological, and biochemical characteristics in patients with fluoroacetic acid poisoning in the emergency department. Hum Exp Toxicol. 2020;39(5):634–41. https://doi.org/10.1177/0960327119897743.
8. Cao F, Lu X, Hu X, Zhang Y, Zeng L, Chen L, et al. In vitro selection of DNA aptamers binding pesticide fluoroacetamide. Biosci Biotech Bioch. 2016;80(5):823–32. https://doi.org/10.1080/09168451.2015.1136876.
9. Wen W, Gao H, Kang N, Lu A, Qian C, Zhao Y. Treatment of severe fluoroacetamide poisoning in patient with combined multiple organ dysfunction syndrome by evidence-based integrated Chinese and Western medicines: a case report. Medicine. 2017;96(27):7265. https://doi.org/10.1097/MD.0000000000007256.
10. Lu A, Yuan F, Yao Y, Wen W, Lu H, Wu S, et al. Reversible leukoencephalopathy caused by 2 rodenticides bromadiolone and fluroacetamide: a case report and literature review. Medicine. 2021;100(9):25053. https://doi.org/10.1097/MD.0000000000025053.
11. Egyed MN. Mass poisoning in dogs due to meat contaminated by sodium fluoro acetate or fluoro acetamide special reference to the differential diagnosis. Fluoride. 1979;12(2):76–84.
12. Jones K. Two outbreaks of fluoroacetate and fluoroacetamide poisoning. J Forensic Sci Soc. 1965;5(2):76–9. https://doi.org/10.1016/S0015-7368(65)70235-1.
13. Shlosberg A, Egyed MN, Mendelssohn H, Langer Y. Fluoroacetamide (1081) poisoning in wild birds. J Wildlife Dis. 1975;11(4):534–6. https://doi.org/10.7589/0090-3558-11.4.534.
14. Zhang D, Zhang J, Zuo Z, Liao L. A retrospective analysis of data from toxic substance-related cases in Northeast China (Heilongjiang) between 2000 and 2010. Forensic Sci Int. 2013;231(1–3):172–7. https://doi.org/10.1016/j.forsciint.2013.05.014.
15. Rong W, Liu H, Chen B, Zhu F, Ji W, Ma Y. Determination of four rodenticides in foods by gas chromatography-tandem mass spectrometry. Chin J Anal Lab. 2013;32(1):73–7. https://doi.org/10.13595/j.cnki.issn1000-0720.2013.0019.
16. Cai X, Zhang D, Ju H, Wu G, Liu X. Fast detection of fluoroacetamide in body fluid using gas chromatography–mass spectrometry after solid-phase microextraction. J Chromatogr B. 2004;802(2):239–45. https://doi.org/10.1016/S1570-0232(03)00556-7.
17. Huang H, Huang X, Yu J. Simultaneous determination of five hypertoxic rodenticides in serum by gas chromatography-mass spectrometry. Chin J Chromatogr. 2015;33(3):323–8.
18. Li Z, Rong W, Chen B, Liu H. Simultaneous determination of fluoroacetamide and tetramine in fresh pork by gas chromatography-mas spectrometry. Jiangsu J Prev Med. 2021;32(6):679–81. https://doi.org/10.13668/j.issn.1006-9070.2021.06.009.
19. Xu X, Song G, Zhu Y, Zhang J, Zhao Y, Shen H, et al. Simultaneous determination of two acute poisoning rodenticides tetramine and fluoroacetamide with a coupled column in poisoning cases. J Chromatogr B. 2008;876(1):103–8. https://doi.org/10.1016/j.jchromb.2008.10.027.
20. Cooney TP, Varelis P, Bendall JG. High-throughput quantification of monofluoroacetate (1080) in milk as a response to an extortion threat. J Food Protect. 2016;79(2):273–81. https://doi.org/10.4315/0362-028X.JFP-15-405.
21. Liu L, Hu S, Zhai S, Hai X. Analysis of monofluoroacetic acid in human plasma by UFLC–MS/MS and its application in patients with sodium monofluoroacetate or monofluoroacetamide poisoning. J Pharmaceut Biomed. 2018;158:370–5. https://doi.org/10.1016/j.jpba.2018.06.028.
22. Yang L, Zhang X, Shen D, Yu X, Li Y, Wen K, et al. Hapten design and monoclonal antibody to fluoroacetamide, a small and highly toxic chemical. Biomolecules. 2020;10(7):986. https://doi.org/10.3390/biom10070986.
23. Fjordbøge AS, Uthuppu B, Jakobsen MH, Fischer SV, Broholm MM. Mobility of electrostatically and sterically stabilized gold nanoparticles (AuNPs) in saturated porous media. Environ Sci Pollut R. 2019;26(28):29460–72. https://doi.org/10.1007/s11356-019-06132-8.
24. Kong D, Liu L, Song S, Suryoprabowo S, Li A, Kuang H, et al. A gold nanoparticle-based semi-quantitative and quantitative ultrasensitive paper sensor for the detection of twenty mycotoxins. Nanoscale. 2016;8(9):5245–53. https://doi.org/10.1039/C5NR09171C.

Publisher's Note